

Lanthanide Coordination Polymers

Two Series of Lanthanide Coordination Polymers and Complexes with 4'-Phenylterpyridine and their Luminescence Properties

Alexander E. Sedykh,^[a,b] Dirk G. Kurth,^[c] and Klaus Müller-Buschbaum^{*[a,b]}

Abstract: Two series of trivalent lanthanide and group 3 metal coordination polymers with 4'-phenyl-2,2':6',2''-terpyridine (ptpy) of the composition $1_{\infty}[\text{MCl}_3(\text{ptpy})]$ (**1**, M = La, Ce, Pr, Nd) and the complexes $[\text{MCl}_3(\text{ptpy})(\text{py})]$ (**2**, M = Pr, Nd, Sm, Eu, Gd, Tb, Dy, Ho, Er, Tm, Yb, Lu, Y) have been synthesized and characterized. For europium, the complex $[\text{Eu}_2\text{Cl}_6(\text{ptpy})_2]$ (**3**) was obtained as single crystals, its dimeric structure providing potential insight into the coordination polymer formation from monomeric entities. Product series **1** and **2** were photophysically investigated in the solid state at room temperature and

77 K. Alongside with standard ion-specific 4f–4f trivalent lanthanide luminescence in the visible and NIR (of emitters such as europium, terbium, dysprosium, neodymium, etc.), visible range emission of praseodymium, holmium, erbium, and thulium was observed, which is rarely reported for coordination compounds. It occurs in addition to their characteristic NIR emission. For complexes of series **1**, an exciplex based luminescence was observed originating from ligand π -stacking in the crystal packing.

Introduction

Trivalent lanthanides are known for their luminescent properties with characteristic emission for each metal ion.^[1–3] They emit throughout the visible and NIR, and some of the typical NIR emitters also have possible transitions in the visible range,^[4,5] but these are usually too weak to be readily observed. Terpyridine and its derivatives are known to enhance trivalent lanthanide luminescence, but mostly photophysical properties of these compounds are well studied for the standard visible emitters, such as Eu^{3+} ^[6–14] and Tb^{3+} ^[8–14] whereas other rare earth metal ions such as Er^{3+} ^[13–16] or Tm^{3+} ^[17] have been investigated to a lesser extent. For the ligand 4'-phenyl-2,2':6',2''-terpyridine (ptpy), complexes especially with transition metals were studied.^[18–24] Several examples of ptpy coordination compounds with rare earth metal ions are known, typically for

La^{3+} ,^[25,26] Nd^{3+} ,^[27] Eu^{3+} ,^[28–30] Gd^{3+} ,^[25,26,28,30] Tb^{3+} ,^[28,30] Dy^{3+} ,^[30] Lu^{3+} .^[28]

We present that lanthanide and group 3 metal coordination compounds with 4'-phenyl-2,2':6',2''-terpyridine (ptpy) can be obtained at elevated temperatures as coordination polymers and as complexes at lower synthesis temperatures, covering the complete lanthanide series (Figure 1) and describe ion specific 4f-based luminescence for complexes and coordination polymers as well as possible exciplex formation.

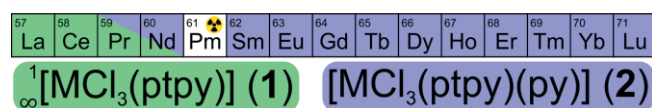


Figure 1. Accessibility of coordination polymers and complexes obtained in reactions of trivalent lanthanide chlorides and ptpy in pyridine.

Results and Discussion

Synthesis and Structural Analysis

The series of coordination polymers $1_{\infty}[\text{MCl}_3(\text{ptpy})]$ (**1**) and complexes $[\text{MCl}_3(\text{ptpy})(\text{py})]$ (**2**) form in reactions of anhydrous lanthanide and group 3 metal chlorides with ptpy in pyridine with excellent yield (Scheme 1). For the first elements of the lanthanide series (La till Nd), a polymeric structure is accessible, whereas for the smaller lanthanide and group 3 metal ions (Y, Pr till Lu, excluding Pm) isotypic complexes are formed. A change of the degree of aggregation of the structures is observed for Pr^{3+} and Nd^{3+} , as for both, coordination polymers and complexes can be obtained.

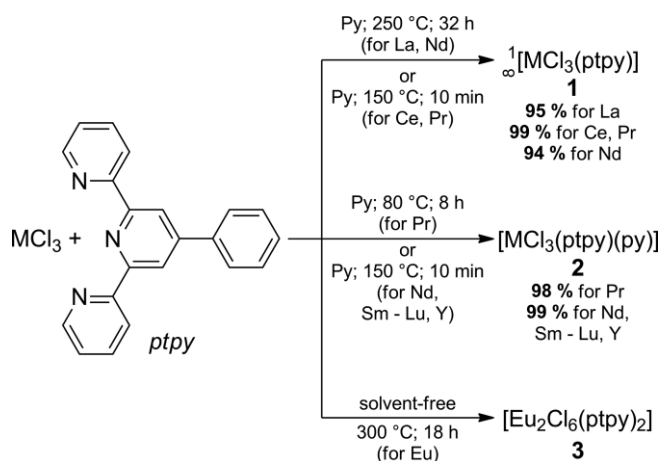
[a] Institute of Inorganic and Analytical Chemistry, Justus-Liebig-University Giessen, Heinrich-Buff-Ring 17, 35392 Giessen, Germany
E-mail: kmbac@uni-giessen.de
<https://www.uni-giessen.de/fbz/fb08/Inst/iaac/mueller-buschbaum>

[b] Institute of Inorganic Chemistry, Julius-Maximilians-University Würzburg, Am Hubland, 97074 Würzburg, Germany

[c] Lehrstuhl für Chemische Technologie der Materialsynthese, Julius-Maximilians-University Würzburg, Röntgenring 11, 97070 Würzburg, Germany

Supporting information and ORCID(s) from the author(s) for this article are available on the WWW under <https://doi.org/10.1002/ejic.201900872>.

© 2019 The Authors. Published by Wiley-VCH Verlag GmbH & Co. KGaA. This is an open access article under the terms of the Creative Commons Attribution-NonCommercial License, which permits use, distribution and reproduction in any medium, provided the original work is properly cited and is not used for commercial purposes.



Scheme 1. Synthesis of $1[MCl_3(ptpy)(py)]$ (**1**), $[MCl_3(ptpy)(py)]$ (**2**), and single crystal of $[Eu_2Cl_6(ptpy)_2]$ (**3**).

In $1[MCl_3(ptpy)]$ (**1**, M = La, Ce, Pr, Nd), crystallizing in orthorhombic space group *Pbca*, the metal centre has a CN of eight, being coordinated by five chlorides and ptpy, forming a distorted triangular dodecahedron. Metal ions are connected with each other through two chlorides, forming an infinite one-dimensional chain, where each following ptpy points in the opposite direction (Figure 2).

All complexes $[MCl_3(ptpy)(py)]$ (**2**, M = Pr, Nd, Sm, Eu, Gd, Tb, Dy, Ho, Er, Tm, Yb, Lu, Y) are isotypic, also crystallizing in the orthorhombic space group *Pbca*, and the metal centre has a CN of seven, being coordinated by three chlorides, one pyridine and a slightly twisted ptpy ligand, forming a distorted pentagonal bipyramid (Figure 3a). For all complexes of constitution **2**, except for **2-Pr**, it was possible to obtain single crystals and analyse them. With reduction of the ionic radius of the metal centre^[31] (and therefore increase of the charge density), interatomic distances to coordinated atoms decrease (Figure 3c). Interatomic distances between metal and chloride ions and metal and ptpy nitrogen atoms remain in the same relative order, while the distance between metal and the pyridine nitrogen atom (Figure 3b, black line) is the longest among M–N bonds

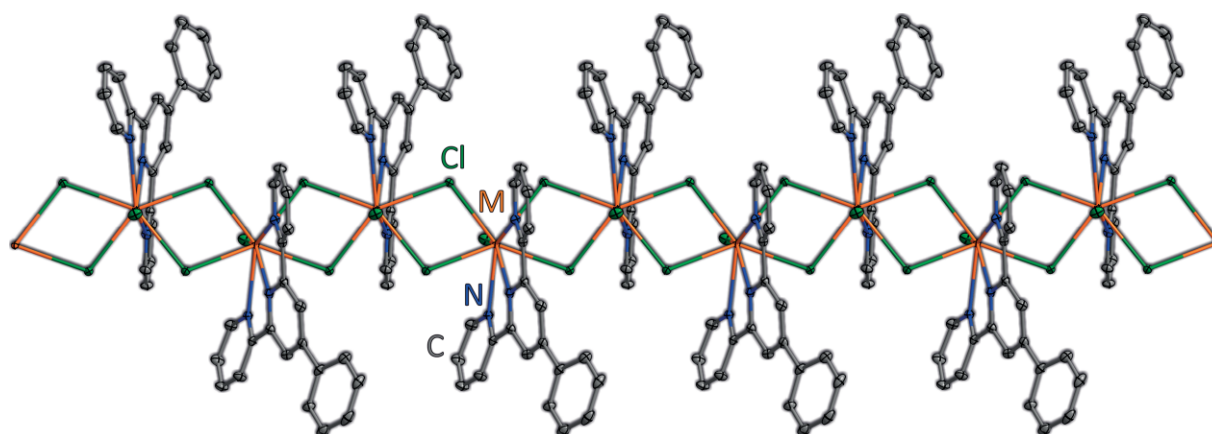


Figure 2. Selected view of the X-ray crystal structure of $1[MCl_3(ptpy)]$ (**1**). Thermal ellipsoids describe 50 % probability level of the atoms; hydrogen atoms are omitted (M orange, Cl green, C grey, N blue).

for the beginning of the lanthanide row and in the end it is shorter than the ones of ptpy side rings. This can be explained by the rigid main ligand structure, whereas the pyridine could move more freely in the coordination sphere.

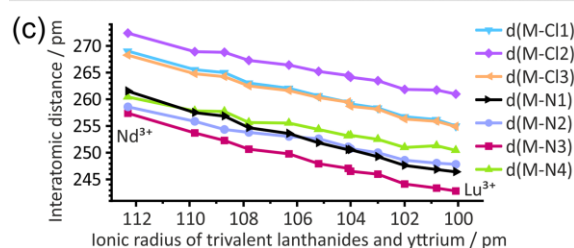
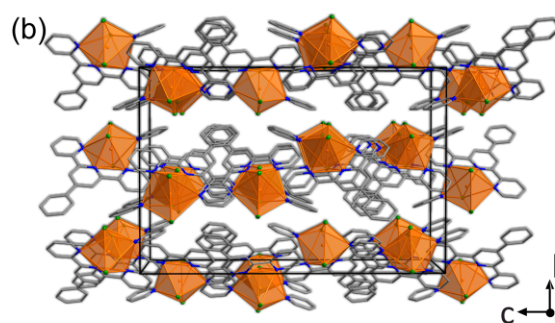
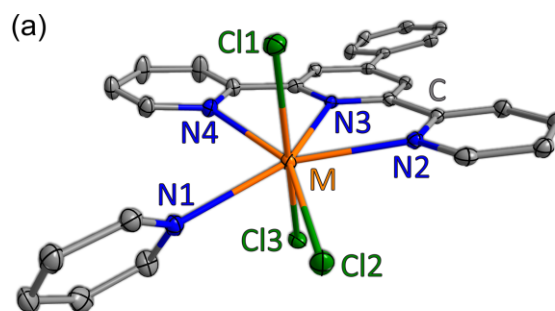


Figure 3. (a) and (b): X-ray crystal structure of a complex unit and a unit cell view of $[MCl_3(ptpy)(py)]$ (**2**). Thermal ellipsoids describe a 50 % probability level of the atoms; hydrogen atoms are omitted (M orange, Cl green, C grey, N blue). (c): dependence of the interatomic distances in the crystal structure of **2** (M = Nd, Sm – Lu, Y) on metal ion radii.

It was possible to also obtain single crystals of the dimeric complex $[\text{Eu}_2\text{Cl}_6(\text{ptpy})_2]$ (**3**) in a solvent-free reaction between EuCl_3 and ptpy (Scheme 1). Unfortunately, upscaling of this synthesis has proved to be unsuccessful, so a characterisation of this compound fully by other analytics was unattainable. Nonetheless, an insight in the structure of the dimeric complex **3** provides valuable information on the formation of the polymeric structure **1** via dimeric and possibly also oligomeric units. The dimer **3** crystallizes in the monoclinic space group $P2_1/c$, with Eu^{3+} having a CN of seven and being coordinated by ptpy and four chloride ions, of which two are bridging; with each of europium having a distorted pentagonal bipyramid coordination polyhedron (Figure 4a). Such a dimeric complex is the next logic step in connecting monomeric complexes, such as **2**, and coordination polymers, such as **1**, as upon composition of the latter at first dimers and oligomers should be formed, which subsequently form a polymer. Naturally, those dimers could have a structure different from **3**, but nevertheless its existence shows a transition path from monomeric complexes to coordination polymers.

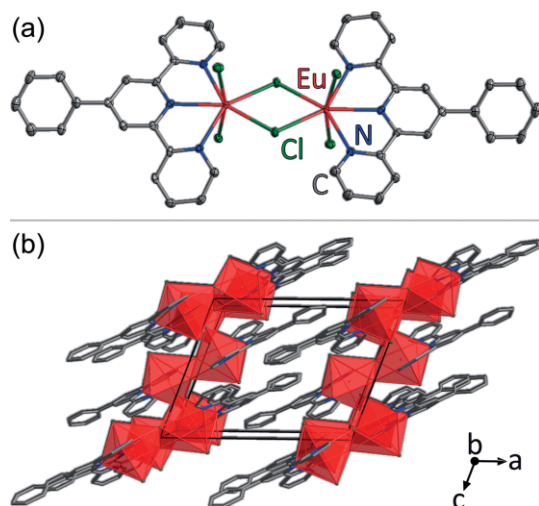


Figure 4. A X-ray crystal structure of a complex unit and a unit cell view of $[\text{Eu}_2\text{Cl}_6(\text{ptpy})_2]$ (**3**). Thermal ellipsoids describe a 50% probability level of the atoms; hydrogen atoms are omitted (Eu red, Cl green, C grey, N blue).

Details on coordination spheres bond lengths and angles for each compound could be found in the SI.

Photophysical Properties

The coordination polymers **1**, namely **1-La**, **1-Nd**, and **1-Pr**, exhibit ligand based excitation and emission and show 4f-metal ion based emission for **1-Pr** only in the visible, and for **1-Nd** in the NIR (Figure 5). For **1-Ce**, a broad metal-based emission band additional to the ligand emission band could be observed as a shoulder in the spectrum at higher energy (Figure 5 – Ce). This band originates from 5d–4f transitions of the Ce^{3+} . Both ligand and Ce^{3+} emission have excitation below 300 nm, which corresponds to 4f–5d excitation of the metal ion,^[32,33] meaning that energy can also be transferred from Ce^{3+} to the ligand. However, the emission intensity of **1-Ce** is low and cannot be ob-

served by a naked eye; it can be detected only by the photoluminescence spectrometer – which is a result of Ce^{3+} and ligand energy levels close position and, therefore, quenching of the luminescence by forth and back energy transfer.

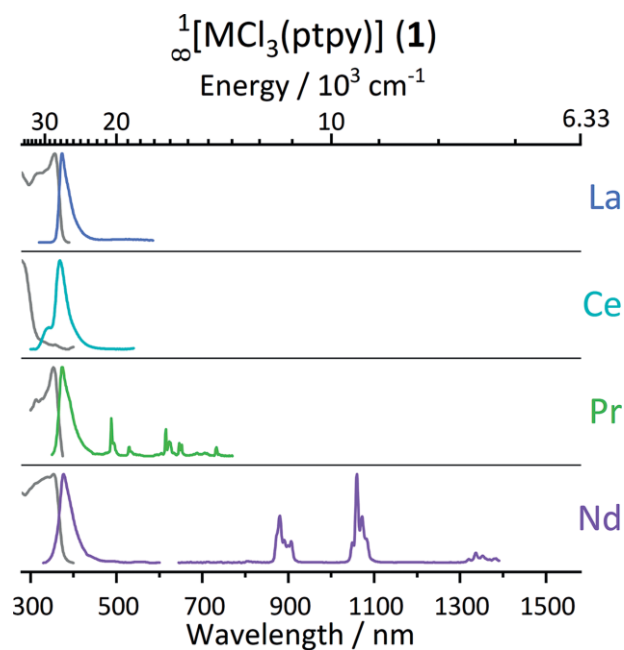


Figure 5. Room temperature solid state normalized excitation (grey) and emission spectra (coloured, $\lambda_{\text{ex}} = 280, 310, 335, \text{ or } 355 \text{ nm}$) of $1-\infty[\text{MCl}_3(\text{ptpy})]$ (**1**). Visible and NIR emission spectra for **1-Nd** were normalized separately.

Excitation, ligand and metal ion based emission spectra of complexes **2** in the visible and NIR range are presented in Figure 6. The complexes with Ln^{3+} 4f–4f emitters have excitation spectra similar to the **2-Y**, **2-Lu**, and **2-Gd** products with a maximum around 365 nm for all complexes (Figure 6), indicating that the ligand is responsible for the light uptake. Both excitation and emission of the ligand in **2** are bathochromically shifted by ca. 10 nm in comparison with **1**. For **2-Gd**, an emission from the ligand triplet state is already visible at room temperature (Figure 6 – Gd) and at 77 K it becomes more intense and better resolved, allowing to determine its energy level from the shortest wavelength phosphorescence band at approximately 21100 cm^{-1} (Figure S39). Metal ion emission of **2-Eu** is so intense that not only the transitions from the lowest excited state ($^5\text{D}_0 \rightarrow ^7\text{F}_j$) are observed, but also from a higher level ($^5\text{D}_1 \rightarrow ^7\text{F}_j$, Figure 6 – Eu, inset). Furthermore, Eu^{3+} emission was observed also in the emission spectra of **2-Gd**, **2-Dy**, **2-Er**. However, its content was estimated to be below 1 ppm, which is described in detail in the SI (see section on doping experiments), and it originates from starting lanthanide source – similar issue was reported before for Gd^{3+} complex with a comparable ligand.^[34] Other typical visible region emitters, such as Sm^{3+} , Tb^{3+} , and Dy^{3+} also show their characteristic emission. In addition, **2-Sm** and **2-Dy** show NIR emission bands, alongside with NIR emission of **2-Pr**, **2-Nd**, **2-Ho**, **2-Er**, **2-Tm**, and **2-Yb** (Figure 6). It is remarkable that **1-Pr**, **2-Pr**, **2-Ho**, **2-Er**, and **2-Tm** show their characteristic ion-specific 4f–4f emission in the visi-

ble range at room temperature, which has been well studied for doped inorganic materials,^[35–42] whereas for coordination compounds these transitions in the solid state are rarely re-

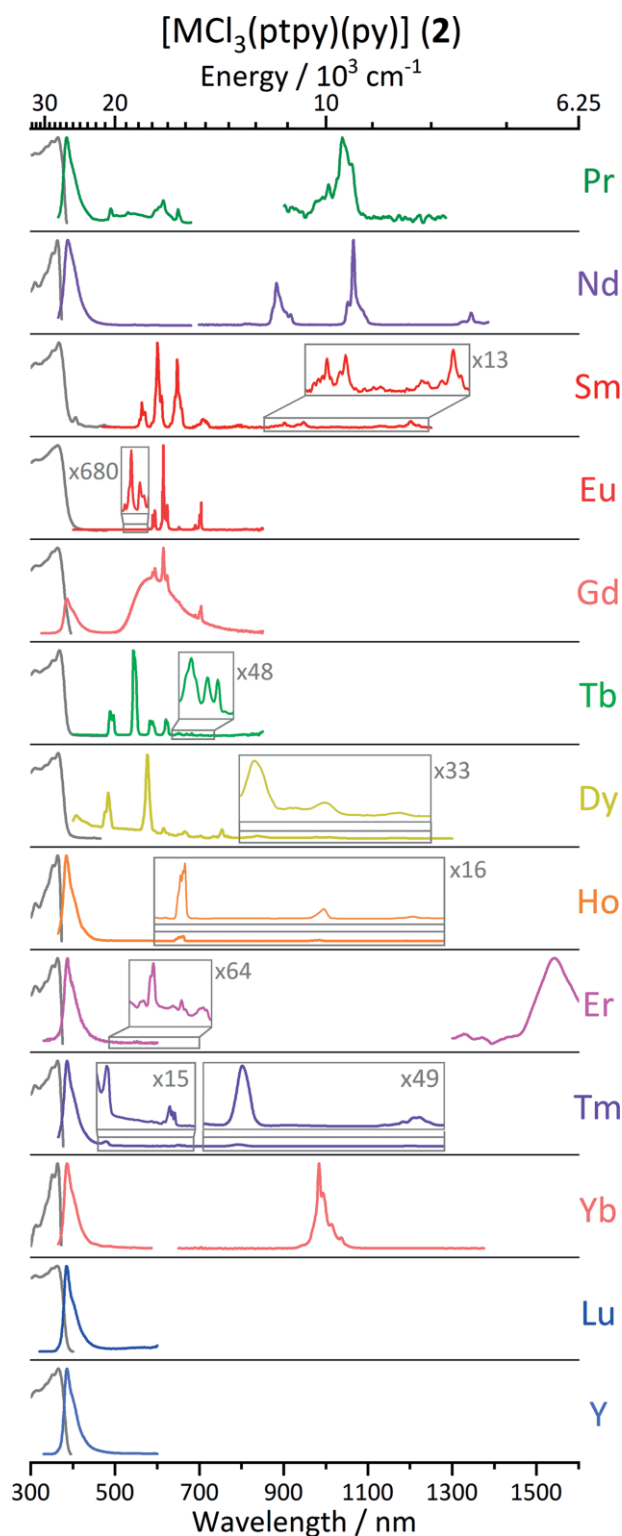


Figure 6. Room temperature solid state normalized excitation (grey) and emission spectra (coloured, $\lambda_{\text{ex}} = 310$ or 365 nm) of $[\text{MCl}_3(\text{ptypy})(\text{py})]$ (**2**). Emission spectra in the visible and NIR for **2-Pr**, **2-Nd**, **2-Er**, and **2-Yb** were normalized separately.

ported, possibly due to low intensities. Emission of Pr^{3+} , Ho^{3+} , and Tm^{3+} at room temperature in the visible range is promoted through ligand sensitization in complexes with pyrazole and hexafluoroacetylacetonate,^[43] 3-hydroxypyridin-2-one,^[44] $\text{N,N}'$ -bis(1-phenylethyl)-2,6-pyridine-dicarboxamide,^[45] or bis-tetrazolate-pyridine.^[46] However, only the latter sensitizes all three mentioned metal ions. For Er^{3+} coordination compounds, metal ion based emission in the visible range through the ligand excitation was noticed upon cooling below 200 K^[47] or at 3 K,^[15,48,49] and only as exceptions, this phenomenon was observed at room temperature.^[15,16,50] For each compound, enlarged detailed spectra measured at room temperature and 77 K with Designation of observed emission bands with Ln^{3+} 4f–4f transitions are reported in the SI.

Quantitative luminescence data – emission lifetimes by overall process decay times and quantum yields – of the coordination compounds presented were collected for all cases with suitable emission intensity (Table 1). The photophysical properties of the obtained Tb^{3+} and Eu^{3+} compounds are comparable to other terpyridine derivative complexes, e.g. for Eu^{3+} showing lifetimes > 1 ms and significant quantum yields in the solid state $> 50\%$ ^[8–11,28] (**2-Eu**: $1410(1)$ μs , $55.2(7)\%$), while for Tb^{3+} , lifetimes and quantum yields in combination with sensitizers of equal energy range as ptpy are typically lower than for Eu^{3+} ^[10,11,28] (**2-Tb**: $349(3)$ μs , $12.8(3)\%$). For **2-Sm**, the luminescence lifetime is shorter ($33.82(3)$ μs , $\text{QY} < 1\%$) and well in the range of other complexes of Sm^{3+} .^[51–58] Quantum yields of the Dy^{3+} , Pr^{3+} , Ho^{3+} , and Tm^{3+} products obtained could not be determined reliably due to low intensity of emission in the visible, and of Nd^{3+} and Yb^{3+} products due to emission in the NIR. However, the respective metal ion based emission lifetimes were also successfully determined for the Dy^{3+} , Pr^{3+} , Ho^{3+} , Tm^{3+} , and Yb^{3+} products (Table 1), which are also close to the values presented in the literature.^[13,58–69]

Table 1. Photophysical data of ptpy, $[\infty\text{MCl}_3(\text{ptypy})]$ (**1**), and $[\text{MCl}_3(\text{ptypy})(\text{py})]$ (**2**) in the solid state at room temperature.

Compound	τ ^[a]	$\lambda_{\text{ex}}/\lambda_{\text{em}}$ [nm] ^[b]	Φ [%] ^[c]	$\lambda_{\text{ex}}/\lambda_{\text{em}}$ [nm] ^[d]
ptypy	2.728(6) ns ^[e]	316/374	18.2(2)	330/340–500
2-Y	1.22(4) ns ^[e]	316/385	9.8(5)	330/340–550
1-La	1.19(6) ns ^[e]	316/373	13.1(3)	330/345–500
1-Pr	1.31(2) μs ^[f]	377/622	n/a	n/a
2-Pr	1.03(7) μs ^[f]	377/614	n/a	n/a
1-Nd	< 2 μs ^[f,g]	350/1060	n/a	n/a
2-Nd	< 2 μs ^[f,g]	360/1066	n/a	n/a
2-Sm	33.82(3) μs ^[f]	360/600	0.69(1)	365/545–735
2-Eu	1410(1) μs ^[f]	365/614	55.2(7)	365/570–715
2-Gd	< 1 ns ^[e,g]	316/386	0.39(1)	330/355–475
	628(17) μs ^[h]	364/550	3.5(2)	330/475–775
2-Tb	349(43) μs ^[f]	360/543	12.8(3)	365/480–660
2-Dy	2.67(9) μs ^[f]	365/576	n/a	n/a
2-Ho	1.3(3) μs ^[f]	377/657	n/a	n/a
2-Tm	1.26(2) μs ^[f]	377/651	n/a	n/a
2-Yb	10.69(4) μs ^[f]	360/983	n/a	n/a

[a] Emission lifetime. [b] Excitation and emission wavelengths of emission lifetime measurement. [c] Quantum yield. [d] Excitation wavelength and emission range of QY measurement. [e] Singlet state emission of the ligand. [f] 4f–4f emission of the metal ion. [g] Lifetime is below the instrumental measurement limit. [h] Triplet state emission of the ligand.

Emission lifetimes were determined at low temperature as well; detailed data can be found in the SI. The most significant changes in emission lifetimes between r.t. and 77 K can be observed for complexes of **2-Tb** and **2-Dy**, for which an increase by more than 5 times compared to r.t. decay times was observed at 77 K (**2-Tb**: 2249(2) μ s, **2-Dy**: 14.0(3) μ s). This occurs not only because of the temperature quenching reduction, but also due to decrease of back energy transfer from the excited state of a metal ion to energy levels of the ligand upon cooling. For **2-Tb**, emission decay times were determined temperature dependent in a range of 77 to 298 K: the emission lifetime significantly increases upon cooling down to 150 K and remains almost unchanged upon further cooling (Figure 7).

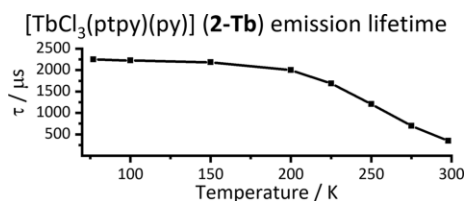


Figure 7. Temperature dependency of **2-Tb** solid state emission lifetime ($\lambda_{\text{ex}} = 360$ nm, $\lambda_{\text{em}} = 543$ nm).

Ligand Exciplex

Additional emission bands were observed in the spectra of the **2-Pr**, **2-Ho**, **2-Er**, and **2-Tm** at 77 K (Figure 9). Though their actual origin and nature cannot be determined unambiguously, we assume that this may be an exciplex ligand emission as result of the complex crystal packing. As shown in Figure 8, intramolecular distances between aromatic rings from different ligands are rather short, and this can be considered as π -stacking, which may lead to an exciplex formation. In all spectra mentioned, this band shows excitation in the region of ligand singlet state emission, and reabsorption of the light by the respective Ln^{3+} could be observed by indentions in the emission spectra, most noticeably in the case of **2-Ho** and **2-Er** (Figure 9). Emission lifetime of this additional ligand emission was determined exemplarily for **2-Ho** to be on the nanosecond scale (3.00(1) ns at 77 K). This emission could even be noticed at room temperature in the spectra of **2-Pr** (SI Figure S30) and weakly for **2-Ho** (SI Figure S46).

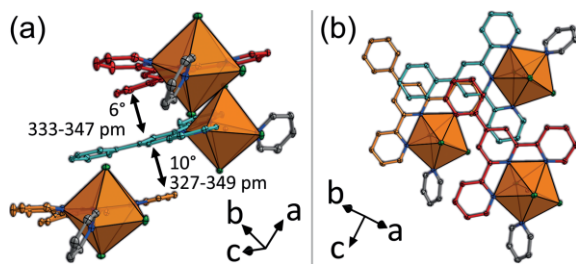


Figure 8. Selected views of the X-ray crystal structure of **2-Er** indicating the possibility of an excimer formation. Thermal ellipsoids describe 50 % probability level of the atoms (Er orange, Cl green, grey/red/turquoise/magenta, N blue). Hydrogen atoms are omitted.

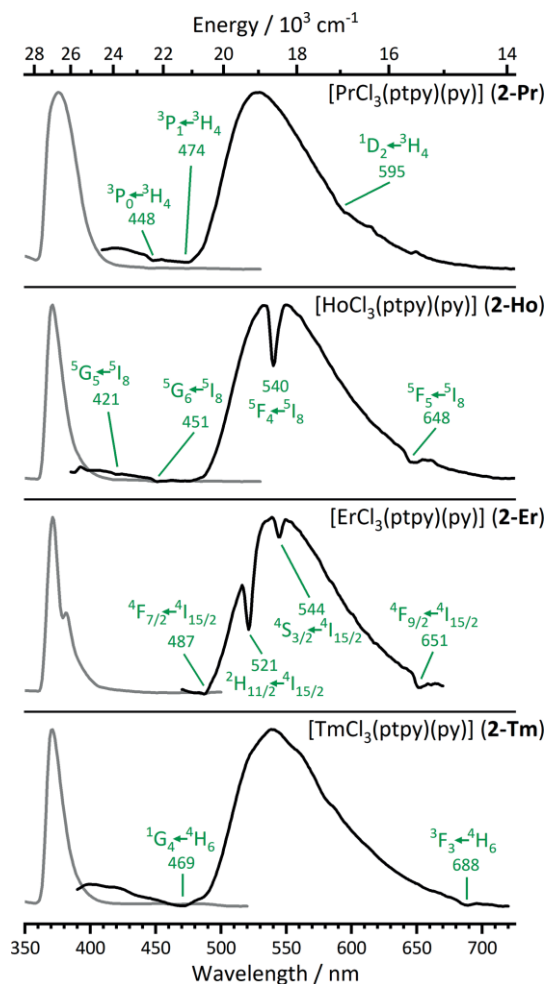


Figure 9. Low temperature (77 K) solid state normalized excitation (grey, $\lambda_{\text{em}} = 550$ nm) and emission spectra (black, $\lambda_{\text{ex}} = 370$ nm) of **2-Pr**, **2-Ho**, **2-Er**, **2-Tm** additional ligand-based luminescence.

Conclusions

In summary, thirteen trivalent lanthanide and group 3 metal chloride complexes and four coordination polymers with 4'-phenyl-2,2':6',2''-terpyridine were synthesized and characterized. They exhibit luminescence, with the ligand absorbing light in the UV region, the energy being transferred to the metal ion centre, leading to Ln^{3+} -based 4f–4f emission in the visible and NIR region. This further includes luminescence rarely reported for coordination compounds of typical NIR emitters in the visible range, such as Pr^{3+} , Ho^{3+} , Er^{3+} , and Tm^{3+} . In addition, exciplex based emission has been observed. Furthermore, isolation of a dimeric Eu^{3+} complex with pty provides an insight into the first step of coordination polymers formation from the respective monomeric entities.

Experimental Section

Analytical Methods

CHN Analysis: For carbon, hydrogen, and nitrogen elemental analysis the compounds were placed in a tin crucible with at least one mass equivalent of V_2O_5 ; samples were stored under inert condi-

tions prior to the measurements. Analyses were performed using a Vario Micro Cube (Elementar Analysensysteme GmbH).

Single Crystal X-ray Diffraction: Single crystals of the corresponding products were mounted on a goniometer head using a perfluorinated ether (viscosity 1800 cSt, 99.9 %, ABCR). Data collection was performed using Mo- $K_{\alpha 1}$ X-ray radiation with a BRUKER AXS Apex II diffractometer at 100 K with a Helios-mirror or Graphite monochromator using the BRUKER AXS.^[70] Data processing was accomplished with XPREP.^[71] All structure solutions were carried out with direct methods using SHELXT^[72] and the obtained crystal structures were refined with least square techniques using SHELXL^[73] on the graphical platform shelXle.^[74]

CCDC 1895773 (for **1-La**), 1895774 (for **1-Ce**), 1895775 (for **1-Pr**), 1895776 (for **1-Nd**), 1895777 (for **3**), 1822581 (for **2-Nd**), 1822582 (for **2-Sm**), 1822583 (for **2-Eu**), 1822584 (for **2-Gd**), 1822585 (for **2-Tb**), 1822586 (for **2-Dy**), 1822587 (for **2-Ho**), 1822588 (for **2-Er**), 1822589 (for **2-Tm**), 1822590 (for **2-Yb**), 1822591 (for **2-Lu**) and 1822592 (for **2-Y**) contain the supplementary crystallographic data for this paper. These data can be obtained free of charge from The Cambridge Crystallographic Data Centre.

Powder X-ray Diffraction: Samples for powder diffraction were grinded in a mortar and filled in mark tubes made of soda lime glass with \varnothing 0.3 mm (Hilgenberg GmbH), which were cut and sealed with picein wax. Diffraction data was collected with a powder X-ray diffractometer BRUKER AXS D8 Discover equipped with a LYNXEYE detector in a transmission geometry. X-ray radiation (Cu- $K_{\alpha 1}$) was focused with a Goebel mirror (Cu- $K_{\alpha 2}$ was eliminated by Ni absorber). Collection and analysis of the data was performed using the BRUKER AXS Difracc.Suite™ software.

Vibrational Spectroscopy: MIR spectra were recorded under non-inert conditions from several milligrams of the compounds with a Nicolet 380 FT-IR spectrometer (ATR module) using OMNIC™ software.

Photoluminescence Spectroscopy: Solid samples were filled in spectroscopically pure quartz glass cuvettes under inert gas atmosphere and examined at room temperature or at 77 K using special liquid nitrogen filled Dewar assembly (FL-1013, HORIBA).

Excitation and emission spectra in UV and visible range (250–850 nm) were recorded with a HORIBA Jobin Yvon Spex Fluorolog 3 spectrometer equipped with a 450 W Xe short-arc lamp (OSRAM), double-grated excitation and emission monochromators, and a photomultiplier tube (R928P) using a FluoroEssence™ software. Both excitation and emission spectra were corrected for the spectral response of the monochromators and the detector using spectra corrections provided by the manufacturer. Additionally, excitation spectra were corrected for the spectral distribution of the lamp intensity by use of a photodiode reference detector. When required, an edge filter (Newport) was used during collection of the data. An Er³⁺ NIR emission spectrum was recorded with a Photon Technology International QuantaMaster™ Model QM-2000–4 spectrometer equipped with a photomultiplier (R928P), an InGaAs-NIR detector, and a 75 W short arc lamp (UXL-75XE, Ushio). Additionally, a filter for excitation (300 nm bandpass, Δ = 20 nm, OD = 5, Edmund Optics) and an edge filter for emission (RG780, Edmund Optics) were applied.

Photoluminescence quantum yields were determined with the above-mentioned HORIBA Jobin Yvon Spex Fluorolog 3 spectrometer equipped with a HORIBA Quanta- ϕ F-3029 Integrating Sphere using a FluoroEssence™ software. For the measurements, solid samples were filled into Starna Micro Cell cuvettes 18-F/ST/C/Q/10 (fluorescence with ST/C closed-cap, material UV quartz glass Spectrosil

Q, pathlength 10 mm, matched). Dry barium sulfate was used as a reference material. Each sample was measured at least three times and the quantum yield values with standard deviation were evaluated afterwards. Quanta- ϕ Integrating Sphere was checked by measuring a standard (sodium salicylate as a powder, λ_{ex} = 340 nm, λ_{em} = 365–600 nm, measured QY = 51.7(1.7) %, in the literature: 53 %).^[75]

Photoluminescence lifetimes were determined using an Edinburgh Instruments FLS920 spectrometer by overall process decay time determination. The decay times were recorded by time-correlated single-photon counting (TCSPC) using a microsecond flash lamp, picosecond pulsed laser diode, or pulsed LEDs for sample excitation. The luminescence emission was collected at right angles to the excitation source, and the emission wavelength was selected with a monochromator and detected by a single-photon avalanche diode (SPAD). Exponential reconvolution or tail fitting were used for calculation of resulting intensity decays calculation using Edinburgh F900 analysis software. The quality of the fit was confirmed by χ^2 values. A nitrogen cryostat OptistatDN (Oxford Instruments) was used for photoluminescence lifetime determinations at 77 K. Additionally, NIR spectra at room temperature and 77 K were recorded also using an Edinburgh Instruments FLS920 spectrometer equipped with NIR PMT detector.

Synthesis and Analytical Data

General Information: All syntheses with participation of lanthanides were performed under inert conditions (argon or nitrogen atmosphere) using vacuum line, gloveboxes (MBraun Labmaster SP, Innovative Technology PureLab), Duran® culture tubes with screw caps, Schlenk tubes, and Duran® glass ampoules (outer \varnothing 10 mm, wall thickness 1 mm). Solvents were dried using standard techniques and stored in flasks with J. Young valve with molecular sieves. Details on the crystallographic data, comparison of simulated and recorded powder XRD patterns, detailed IR bands from ATR-MIR investigations, page size photoluminescence spectra with designated 4f–4f transitions, detailed photoluminescence lifetime and quantum yield data, and doping experiments can be found could be found in the SI (69 pages).

Starting Materials: 4'-phenyl-2,2':6',2''-terpyridine was synthesized as described in the literature.^[76] LaCl₃ (99.9 % Heraeus), CeCl₃ (99.9 %, ABCR), PrCl₃, GdCl₃, DyCl₃, YCl₃ (99.9 %, Strem) were purchased and used as received. LnCl₃ synthesized from oxides Eu₂O₃, Er₂O₃, Tm₂O₃, Yb₂O₃ (99.9 %, RC-Nukor), Nd₂O₃, Sm₂O₃, Tb₄O₇ (99.9 %, Auer-Remy), Ho₂O₃ (99.9 %, Strem), Lu₂O₃ (99.9 %, Chempur), HCl solution (10 mol L⁻¹, reagent grade), and NH₄Cl (99.9 %, Fluka) through ammonium halide route according to the literature,^[77] and then purified by sublimation under vacuum (except for EuCl₃ due to possible decomposition).

Synthesis of ¹∞[LaCl₃(ptpy)] (1-La) and ¹∞[NdCl₃(ptpy)] (1-Nd): Anhydrous LaCl₃ or NdCl₃ (0.1 mmol) and 4'-phenyl-2,2':6',2''-terpyridine (0.105 mmol, 32.5 mg) were mortared together and placed together with pyridine (0.5 mL) in the ampoule made from Duran® glass, which was sealed afterwards. The ampoule was placed in the resistance heating oven with thermal control (Eurotherm 2416), heated to 250 °C within 2 hours, then the temperature was hold for 32 hours. Afterwards, the oven was cooled down to room temperature. Resulting solid product was washed twice with pyridine (1 mL) and dried under vacuum.

1-La ¹∞[LaCl₃(ptpy)]: White solid with violet luminescence. Yield: 52.5 mg (95 %). Elemental analysis calcd. (%) for LaCl₃C₂₁H₁₅N₃: C 45.48, H 2.73, N 7.58; found C 44.95, H 2.83, N 7.37.

1-Nd $^1_{\infty}[\text{NdCl}_3(\text{ptpy})]$: Slightly violet solid. Yield: 52.5 mg (94 %). Elemental analysis calcd. (%) for $\text{NdCl}_3\text{C}_{21}\text{H}_{15}\text{N}_3$: C 45.04, H 2.70, N 7.50; found C 44.78, H 2.69, N 7.64.

Synthesis of $^1_{\infty}[\text{CeCl}_3(\text{ptpy})]$ (1-Ce), $^1_{\infty}[\text{PrCl}_3(\text{ptpy})]$ (1-Pr), and $[\text{MCl}_3(\text{ptpy})(\text{py})]$ (2) (M = Nd, Sm, Eu, Gd, Tb, Dy, Ho, Er, Tm, Yb, Lu, Y): A corresponding anhydrous rare earth metal(III) chloride (0.1 mmol) and 4'-phenyl-2,2':6',2''-terpyridine (0.105 mmol, 32.5 mg) were placed in the Duran® culture tube with a screwcap with hole (and septum). Pyridine (0.5 mL) and a stir bar were added to the mixture of solids. Reaction mixture was heated at 150 °C for 10 minutes upon stirring. Following additions and removals of solvent were performed through the septum. After the reaction, the tube was centrifuged, and the solvent was removed. Next step was repeated twice: toluene (1 mL) was added with following stirring, tube was centrifuged again, and the solvent was removed. The complexes are insoluble in pyridine and could be synthesized with quantitative yield. The synthesis could be easily upscaled to 0.3 mmol of MCl_3 with usage of 0.305 mmol of ligand and 1 mL of pyridine.

1-Ce $^1_{\infty}[\text{CeCl}_3(\text{ptpy})]$: Yellow solid. Yield: 54.9 mg (99 %). Elemental analysis calcd. (%) for $\text{CeCl}_3\text{C}_{21}\text{H}_{15}\text{N}_3$: C 45.38, H 2.72, N 7.56; found C 45.55, H 2.92, N 7.47.

1-Pr $^1_{\infty}[\text{PrCl}_3(\text{ptpy})]$: Slightly green solid. Yield: 55.1 mg (99 %). Elemental analysis calcd. (%) for $\text{PrCl}_3\text{C}_{21}\text{H}_{15}\text{N}_3$: C 45.31, H 2.72, N 7.55 %; found C 45.54, H 2.87, N 7.57.

2-Nd $[\text{NdCl}_3(\text{ptpy})(\text{py})]$: White solid. Yield: 63.1 mg (99 %). Elemental analysis calcd. (%) for $\text{NdCl}_3\text{C}_{26}\text{H}_{20}\text{N}_4$: C 48.87, H 3.15, N 8.77 %; found C 48.76, H 3.25, N 8.62.

2-Sm $[\text{SmCl}_3(\text{ptpy})(\text{py})]$: White solid with weak red luminescence. Yield: 63.7 mg (99 %). Elemental analysis calcd. (%) for $\text{SmCl}_3\text{C}_{26}\text{H}_{20}\text{N}_4$: C 48.4, H 3.12, N 8.68 %; found C 48.55, H 3.22, N 8.57.

2-Eu $[\text{EuCl}_3(\text{ptpy})(\text{py})]$: White solid with intense red luminescence. Yield: 64.0 mg (99 %). Elemental analysis calcd. (%) for $\text{EuCl}_3\text{C}_{26}\text{H}_{20}\text{N}_4$: C 48.28, H 3.12, N 8.66 %; found C 48.50, H 3.35, N 8.52.

2-Gd $[\text{GdCl}_3(\text{ptpy})(\text{py})]$: White solid with orange luminescence. Yield: 64.5 mg (99 %). Elemental analysis calcd. (%) for $\text{GdCl}_3\text{C}_{26}\text{H}_{20}\text{N}_4$: C 47.89, H 3.09, N 8.59 %; found C 48.11, H 3.22, N 8.65.

2-Tb $[\text{TbCl}_3(\text{ptpy})(\text{py})]$: White solid with green luminescence. Yield: 65.2 mg (99 %). Elemental analysis calcd. (%) for $\text{TbCl}_3\text{C}_{26}\text{H}_{20}\text{N}_4$: C 47.77, H 3.08, N 8.57 %; found C 47.86, H 3.15, N 8.48.

2-Dy $[\text{DyCl}_3(\text{ptpy})(\text{py})]$: White solid. Yield: 65.5 mg (99 %). Elemental analysis calcd. (%) for $\text{DyCl}_3\text{C}_{26}\text{H}_{20}\text{N}_4$: C 47.51, H 3.07, N 8.52 %; found C 47.69, H 3.14, N 8.54.

2-Ho $[\text{HoCl}_3(\text{ptpy})(\text{py})]$: White or pink solid, colour depends on the light source (compound shows alexandrite effect). Yield: 65.4 mg (99 %). Elemental analysis calcd. (%) for $\text{HoCl}_3\text{C}_{26}\text{H}_{20}\text{N}_4$: C 47.33, H 3.06, N 8.49 %; found C 47.49, H 3.29, N 8.46.

2-Er $[\text{ErCl}_3(\text{ptpy})(\text{py})]$: Slightly pink solid. Yield: 65.7 mg (99 %). Elemental analysis calcd. (%) for $\text{ErCl}_3\text{C}_{26}\text{H}_{20}\text{N}_4$: C 47.17, H 3.04, N 8.46 %; found C 47.28, H 3.15, N 8.30.

2-Tm $[\text{TmCl}_3(\text{ptpy})(\text{py})]$: White solid. Yield: 65.6 mg (99 %). Elemental analysis calcd. (%) for $\text{TmCl}_3\text{C}_{26}\text{H}_{20}\text{N}_4$: C 47.05, H 3.04, N 8.44 %; found C 46.99, H 3.18, N 8.26.

2-Yb $[\text{YbCl}_3(\text{ptpy})(\text{py})]$: White solid. Yield: mg 66.0 (99 %). Elemental analysis calcd. (%) for $\text{YbCl}_3\text{C}_{26}\text{H}_{20}\text{N}_4$: C 46.76, H 3.02, N 8.39 %; found C 46.75, H 3.04, N 8.33.

2-Lu $[\text{LuCl}_3(\text{ptpy})(\text{py})]$: White solid with blue luminescence. Yield: 66.7 mg (99 %). Elemental analysis calcd. (%) for $\text{LuCl}_3\text{C}_{26}\text{H}_{20}\text{N}_4$: C 46.62, H 3.01, N 8.36 %; found C 46.45, H 3.16, N 8.16.

2-Y $[\text{YCl}_3(\text{ptpy})(\text{py})]$: White solid with blue luminescence. Yield: 57.9 mg (99 %). Elemental analysis calcd. (%) for $\text{YCl}_3\text{C}_{26}\text{H}_{20}\text{N}_4$: C 53.5, H 3.45, N 9.6 %; found C 53.55, H 3.71, N 9.53.

Synthesis of $[\text{PrCl}_3(\text{ptpy})(\text{py})]$ (2-Pr): PrCl_3 (0.15 mmol, 37 mg) and 4'-phenyl-2,2':6',2''-terpyridine (0.155 mmol, 48 mg) were placed in the Duran® culture tube with a screwcap with hole (and septum). Pyridine (0.3 mL) and a stir bar were added to the mixture. The reaction mixture was heated at 80 °C for 8 hours upon stirring. Afterwards, the tube was centrifuged, and the solvent was removed. Then the product was dried under vacuum.

2-Pr $[\text{PrCl}_3(\text{ptpy})(\text{py})]$: Slightly green solid. Yield: 93.8 mg (98 %). Elemental analysis calcd. (%) for $\text{PrCl}_3\text{C}_{26}\text{H}_{20}\text{N}_4$: C 49.12, H 3.17, N 8.81 %; found C 48.85, H 3.29, N 8.76.

Obtaining Single Crystals of 1 and 2: Several milligrams of $^1_{\infty}[\text{MCl}_3(\text{ptpy})]$ (1) or $[\text{MCl}_3(\text{ptpy})(\text{py})]$ (2) and 0.5 mL of pyridine were sealed in an ampoule made from Duran® glass. The ampoule was placed in the resistance heating oven with thermal control (Eurotherm 2416), heated to 200 °C within 0.5 hours, then the temperature was hold for 8 hours. Afterwards, the oven was cooled down to room temperature. Resulting crystals were washed two times with toluene, dried under vacuum, and then used for single crystal XRD measurement. Single crystals could be obtained for all products except for 2-Pr. Suitable single crystals of 1-La and 1-Nd were already obtained at the synthesis conditions described before.

Synthesis of $[\text{Eu}_2\text{Cl}_6(\text{ptpy})_2]$ (3): EuCl_3 (0.005 mmol, 1.3 mg) and 4'-phenyl-2,2':6',2''-terpyridine (0.05 mmol, 15.5 mg) were sealed in an ampoule made from Duran® glass. The ampoule was placed in the resistance heating oven with thermal control (Eurotherm 2416), heated to 300 °C within 1 hours, then the temperature was hold for 18 hours. Afterwards, the oven was cooled down to room temperature. Resulting crystals were washed two times with toluene, dried under vacuum, and then used for single crystal XRD measurement.

Acknowledgments

A. E. Sedykh gratefully acknowledges the *Studienstiftung des deutschen Volkes* for a PhD fellowship. The authors acknowledge Stephanie Maaß (Chemical Technology of Advanced Materials, Julius-Maximilians-Universität Würzburg) for the synthesis of 4'-phenyl-2,2':6',2''-terpyridine.

Keywords: Coordination polymers · Lanthanides · Luminescence · N ligands · Optical properties

- [1] S. V. Eliseeva, J.-C. G. Bünzli, *Chem. Soc. Rev.* **2010**, *39*, 189–227.
- [2] K. Binnemans, *Chem. Rev.* **2009**, *109*, 4283–4374.
- [3] J.-C. G. Bünzli, C. Piguet, *Chem. Soc. Rev.* **2005**, *34*, 1048–1077.
- [4] W. T. Carnall, P. R. Fields, K. Rajnak, *J. Chem. Phys.* **1968**, *49*, 4424–4442.
- [5] P. S. Peijzel, A. Meijerink, R. T. Wegh, M. F. Reid, G. W. Burdick, *J. Solid State Chem.* **2005**, *178*, 448–453.
- [6] D. A. Durham, G. H. Frost, F. A. Hart, *J. Inorg. Nucl. Chem.* **1969**, *31*, 833–838.
- [7] W. E. Silva, M. Freire Belian, R. O. Freire, G. F. de Sá, S. Alves Jr., *J. Phys. Chem. A* **2010**, *114*, 10066–10075.
- [8] H.-R. Mürner, E. Chassat, R. P. Thummel, J.-C. G. Bünzli, *J. Chem. Soc., Dalton Trans.* **2000**, 2809–2816.
- [9] C. Galaup, J. M. Couchet, S. Bedel, P. Tisnès, C. Picard, *J. Org. Chem.* **2005**, *70*, 2274–2284.

- [10] G. F. de Sa, F. R. G. E. Silva, O. L. Malta, *J. Alloys Compd.* **1994**, *207*, 457–460.
- [11] E. S. Andreiadis, R. Demadrille, D. Imbert, J. Pécaut, M. Mazzanti, *Chem. Eur. J.* **2009**, *15*, 9458–9476.
- [12] K. P. Carter, S. J. A. Pope, C. L. Cahill, *CrystEngComm* **2014**, *16*, 1873–1884.
- [13] K. P. Carter, K. E. Thomas, S. J. A. Pope, R. J. Holmberg, R. J. Butcher, M. Murugesu, C. L. Cahill, *Inorg. Chem.* **2016**, *55*, 6902–6915.
- [14] R. J. Batrice, R. L. Ayscue, A. K. Adcock, B. R. Sullivan, S. Y. Han, P. M. Piccoli, J. A. Bertke, K. E. Knope, *Chem. Eur. J.* **2018**, *24*, 5630–5636.
- [15] Y. Suffren, B. Goleosorkhi, D. Zare, L. Guénée, H. Nozary, S. V. Eliseeva, S. Petoud, A. Hauser, C. Piguët, *Inorg. Chem.* **2016**, *55*, 9964–9972.
- [16] B. Goleosorkhi, L. Guénée, H. Nozary, A. Fürstenberg, Y. Suffren, S. V. Eliseeva, S. Petoud, A. Hauser, C. Piguët, *Chem. Eur. J.* **2018**, *24*, 13158–13169.
- [17] J. A. Ridenour, K. P. Carter, C. L. Cahill, *CrystEngComm* **2017**, *19*, 1190–1203.
- [18] G. Schwarz, T. K. Sievers, Y. Bodenthin, I. Hasslauer, T. Geue, J. Koetz, D. G. Kurth, *J. Mater. Chem.* **2010**, *20*, 4142–4148.
- [19] M. A. Bork, H. B. Vibbert, D. J. Stewart, P. E. Fanwick, D. R. McMillin, *Inorg. Chem.* **2013**, *52*, 12553–12560.
- [20] G. Schwarz, S. Maisch, S. Ullrich, J. Wagenhöfer, D. G. Kurth, *ACS Appl. Mater. Interfaces* **2013**, *5*, 4031–4034.
- [21] D. N. Chirdon, W. J. Transue, H. N. Kagalwala, A. Kaur, A. B. Maurer, T. Pintauer, S. Bernhard, *Inorg. Chem.* **2014**, *53*, 1487–1499.
- [22] R. Kaushik, A. Ghosh, D. A. Jose, *J. Lumin.* **2016**, *171*, 112–117.
- [23] S. M. Munzert, G. Schwarz, D. G. Kurth, *Inorg. Chem.* **2016**, *55*, 2565–2573.
- [24] M. J. Bezdek, S. Guo, P. J. Chirik, *Inorg. Chem.* **2016**, *55*, 3117–3127.
- [25] A. Hussain, K. Somyajit, B. Banik, S. Banerjee, G. Nagaraju, A. R. Chakravarty, *Dalton Trans.* **2013**, 42–42, 182–195.
- [26] A. Hussain, S. Gadadhar, T. K. Goswami, A. A. Karande, A. R. Chakravarty, *Eur. J. Med. Chem.* **2012**, *50*, 319–331.
- [27] T. Sarkar, S. Banerjee, S. Mukherjee, A. Hussain, *Dalton Trans.* **2016**, *45*, 6424–6438.
- [28] R. T. Golkowski, N. S. Settineri, X. Zhao, D. R. McMillin, *J. Phys. Chem. A* **2015**, *119*, 11650–11658.
- [29] D. Wang, H. Liu, L. Fan, G. Yin, Y. Hu, J. Zheng, *Synth. Met.* **2015**, *209*, 267–272.
- [30] L. L. Cai, Y. T. Hu, Y. Li, K. Wang, X. Q. Zhang, G. Muller, X. M. Li, G. X. Wang, *Inorg. Chim. Acta* **2019**, *489*, 85–92.
- [31] R. D. Shannon, *Acta Crystallogr., Sect. A* **1976**, *32*, 751–767.
- [32] B. Moine, C. Dujardin, H. Lautesse, C. Pedrini, C. M. Combes, A. Belsky, P. Martín, J. Y. Gesland, *Mater. Sci. Forum* **1997**, *239–241*, 245–248.
- [33] L. Guerbous, O. Krachni, *J. Mod. Opt.* **2006**, *53*, 2043–2053.
- [34] C. Piguët, A. F. Williams, G. Bernardinelli, E. Moret, J. G. Bünzli, *Helv. Chim. Acta* **1992**, *75*, 1697–1717.
- [35] U. Hömmerich, E. E. Nyein, D. Lee, J. Heikenfeld, A. Steckl, J. Zavada, *Mater. Sci. Eng. B* **2003**, *105*, 91–96.
- [36] H. Zhang, X. Fu, S. Niu, G. Sun, Q. Xin, *Solid State Commun.* **2004**, *132*, 527–531.
- [37] R.-J. Xie, M. Mitomo, K. Uheda, F.-F. Xu, Y. Akimune, *J. Am. Ceram. Soc.* **2004**, *85*, 1229–1234.
- [38] Y. K. Sharma, S. S. L. Surana, R. K. Singh, R. P. Dubedi, *Opt. Mater.* **2007**, *29*, 598–604.
- [39] G. K. Das, T. T. Y. Tan, *J. Phys. Chem. C* **2008**, *112*, 11211–11217.
- [40] M. Jiao, N. Guo, W. Lü, Y. Jia, W. Lv, Q. Zhao, B. Shao, H. You, *Dalton Trans.* **2013**, *42*, 12395–12402.
- [41] S. Babu, M. Seshadri, A. Balakrishna, V. Reddy Prasad, Y. C. Ratnakaram, *Phys. B* **2015**, *479*, 26–34.
- [42] M. Venkateswarlu, S. Mahamuda, K. Swapna, M. V. V. K. S. Prasad, A. Srinivasa Rao, S. Shakya, A. Mohan Babu, G. Vijaya Prakash, *J. Lumin.* **2015**, *163*, 64–71.
- [43] Z. Ahmed, K. Iftikhar, *J. Phys. Chem. A* **2013**, *117*, 11183–11201.
- [44] E. G. Moore, G. Szigethy, J. Xu, L. O. Pålsson, A. Beeby, K. N. Raymond, *Angew. Chem. Int. Ed.* **2008**, *47*, 9500–9503; *Angew. Chem.* **2008**, *120*, 9642.
- [45] K. T. Hua, J. Xu, E. E. Quiroz, S. Lopez, A. J. Ingram, V. A. Johnson, A. R. Tisch, A. De Bettencourt-Dias, D. A. Straus, G. Muller, *Inorg. Chem.* **2012**, *51*, 647–660.
- [46] N. Wartenberg, O. Raccurt, E. Bourgeat-Lami, D. Imbert, M. Mazzanti, *Chem. Eur. J.* **2013**, *19*, 3477–3482.
- [47] Y. Suffren, D. Zare, S. V. Eliseeva, L. Guénée, H. Nozary, T. Lathion, L. Aboshyan-Sorgho, S. Petoud, A. Hauser, C. Piguët, *J. Phys. Chem. C* **2013**, *117*, 26957–26963.
- [48] L. Aboshyan-Sorgho, C. Besnard, P. Pattison, K. R. Kittilstved, A. Aebischer, J.-C. G. Bünzli, A. Hauser, C. Piguët, *Angew. Chem. Int. Ed.* **2011**, *50*, 4108–4112; *Angew. Chem.* **2011**, *123*, 4194.
- [49] D. Zare, Y. Suffren, L. Guenee, S. V. Eliseeva, H. Nozary, L. Aboshyan-Sorgho, S. Petoud, A. Hauser, C. Piguët, *Dalton Trans.* **2015**, *44*, 2529–2540.
- [50] A. Nonat, C. F. Chan, T. Liu, C. Platas-Iglesias, Z. Liu, W.-T. Wong, W.-K. Wong, K.-L. Wong, L. J. Charbonnière, *Nat. Commun.* **2016**, *7*, 11978.
- [51] H. Hakala, P. Liitti, J. Peuralahti, J. Karvinen, V.-M. Mukkala, J. Hovinen, *J. Lumin.* **2005**, *113*, 17–26.
- [52] J. M. Stanley, C. K. Chan, X. Yang, R. A. Jones, B. J. Holliday, *Polyhedron* **2010**, *29*, 2511–2515.
- [53] W. X. Li, S. Y. Feng, Y. Liu, J. Zhang, X. D. Xin, B. Y. Ao, Y. J. Li, *J. Lumin.* **2013**, *143*, 746–753.
- [54] A.-L. Wang, D. Zhou, Y.-N. Chen, J.-J. Li, H.-X. Zhang, Y.-L. Zhao, H.-B. Chu, *J. Lumin.* **2016**, *177*, 22–30.
- [55] R. Ilmi, K. Iftikhar, *Polyhedron* **2017**, *127*, 191–202.
- [56] R. J. Batrice, J. A. Ridenour, R. L. Ayscue III, J. A. Bertke, K. E. Knope, *CrystEngComm* **2017**, *19*, 5300–5312.
- [57] A. L. Ramirez, K. E. Knope, T. T. Kelley, N. E. Greig, J. D. Einkauf, D. T. De Lill, *Inorg. Chim. Acta* **2012**, *392*, 46–51.
- [58] P. R. Matthes, J. Nitsch, A. Kuzmanoski, C. Feldmann, A. Steffen, T. B. Marder, K. Müller-Buschbaum, *Chem. Eur. J.* **2013**, *19*, 17369–17378.
- [59] N. Dannenbauer, P. R. Matthes, T. P. Scheller, J. Nitsch, S. H. Zottnick, M. S. Gernert, A. Steffen, C. Lambert, K. Müller-Buschbaum, *Inorg. Chem.* **2016**, *55*, 7396–7406.
- [60] R. J. Batrice, A. K. Adcock, P. M. Cantos, J. A. Bertke, K. E. Knope, *Cryst. Growth Des.* **2017**, *17*, 4603–4612.
- [61] C. Doffek, M. Seitz, *Angew. Chem. Int. Ed.* **2015**, *54*, 9719–9721; *Angew. Chem.* **2015**, *127*, 9856.
- [62] T. Güden-Silber, C. Doffek, C. Platas-Iglesias, M. Seitz, *Dalton Trans.* **2014**, *43*, 4238–4241.
- [63] E. Kreidt, C. Bischof, C. Platas-Iglesias, M. Seitz, *Inorg. Chem.* **2016**, *55*, 5549–5557.
- [64] K. P. Carter, C. H. F. Zulato, E. M. Rodrigues, S. J. A. A. Pope, F. A. Sigoli, C. L. Cahill, *Dalton Trans.* **2015**, *44*, 15843–15854.
- [65] S. B. Meshkova, Z. M. Topilova, D. V. Bol'shoi, N. A. Nazarenko, *J. Appl. Spectrosc.* **2000**, *67*, 893–897.
- [66] V. Singh, V. K. Rai, B. Voss, M. Haase, R. P. S. Chakradhar, D. Thirupathi Naidu, S. H. Kim, *Spectrochim. Acta* **2013**, *109*, 206–212.
- [67] R. Van Deun, P. Nockemann, T. N. Parac-Vogt, K. Van Hecke, L. Van Meerelt, C. Görrler-Walrand, K. Binnemans, *Polyhedron* **2007**, *26*, 5441–5447.
- [68] L. Macalik, J. Hanuza, K. Hermanowicz, W. Oganowski, H. Ban-Oganowska, *J. Alloys Compd.* **2000**, *300–301*, 377–382.
- [69] L. Macalik, J. Hanuza, K. Hermanowicz, W. Oganowski, H. Ban-Oganowska, *J. Alloys Compd.* **2000**, *300–301*, 383–388.
- [70] *Apex 2 Suite*, BRUKER AXS Inc., Madison, WI, USA, **2014**.
- [71] XPREP (Version **2014/7**), Program for Symmetry Analysis and Data Reduction of Diffraction Experiments, Bruker AXS Inc., Madison, WI, USA, **2014**.
- [72] G. M. Sheldrick, *Acta Crystallogr., Sect. C Struct. Chem.* **2015**, *71*, 3–8.
- [73] G. M. Sheldrick, *Acta Crystallogr., Sect. A Found. Crystallogr.* **2008**, *64*, 112–122.
- [74] C. B. Hübschle, G. M. Sheldrick, B. Dittrich, *J. Appl. Crystallogr.* **2011**, *44*, 1281–1284.
- [75] M. S. Wrighton, D. S. Ginley, D. L. Morse, *J. Phys. Chem.* **1974**, *78*, 2229–2233.
- [76] J. Wang, G. Hanan, *Synlett* **2005**, *2005*, 1251–1254.
- [77] G. Meyer, E. Garcia, J. D. Corbett, *Inorg. Synth.* **1989**, 146–150.

Received: August 13, 2019